RadioGraphics

CT and MR Imaging of the Inner Ear and Brain in Children with Congenital Sensorineural Hearing Loss[1]

Varsha M. Joshi, DNB • Shantanu K. Navlekar, DMRD • G. Ravi Kishore, MBBS • K. Jitender Reddy, MD • E. C. Vinay Kumar, MS

CME FEATURE

See www.rsna.org/education/rg_cme.html

LEARNING OBJECTIVES FOR TEST 3

After completing this journal-based CME activity, participants will be able to:

- Describe the CT and MR imaging features of inner ear malformations by using standard nomenclature and classification systems.
- Discuss the role of CT and MR imaging in the evaluation of sensorineural hearing loss in children.
- List brain abnormalities that may be associated with congenital sensorineural hearing loss.

TEACHING POINTS

See last page

Imaging plays an important role in the evaluation of congenital sensorineural hearing loss. In children who are candidates for cochlear implantation surgery, it provides vital preoperative information about the inner ear, the vestibulocochlear nerve, and the brain. High-resolution computed tomography (CT) and magnetic resonance (MR) imaging provide excellent delineation of the intricate anatomy of the inner ear: CT depicts the minute details of osseous structures, and MR imaging allows visualization of the fluid-filled spaces and the vestibulocochlear nerve. Together, these complementary modalities can aid decision making about the best management strategy by facilitating the identification and characterization of inner ear malformations and any associated neurologic abnormalities. It is important that the radiologist be familiar with the key imaging features when interpreting CT and MR images obtained in this patient group.

A broad spectrum of inner ear malformations have been described and linked to developmental insults at different stages of embryogenesis, and various systems have been proposed for classifying them. In this article, these malformations are described by using classification systems used by otolaryngologists for ease of interpretation. The relevant normal anatomy and development of the inner ear are briefly surveyed, standard imaging protocols for studying the inner ear are reviewed, and the imaging appearances of frequently observed inner ear malformations are described and illustrated. The impact of the identification of these malformations and commonly associated brain abnormalities on clinical management and prognosis also is discussed.

Abbreviation: IAC = internal auditory canal

RadioGraphics 2012; 32:683–698 • **Published online** 10.1148/rg.323115073 • **Content Codes:** HN NR PD

[1]From the Departments of Radiology (V.M.J., S.K.N., G.R.K., K.J.R.) and ENT (E.C.V.K.), Apollo Hospital, Jubilee Hills, Hyderabad 500 033, India. Recipient of a Certificate of Merit award for an education exhibit at the 2010 RSNA Annual Meeting. Received April 5, 2011; revision requested August 2 and received September 30; accepted November 7. For this journal-based CME activity, the authors, editor, and reviewers have no relevant relationships to disclose. **Address correspondence to** V.M.J. (e-mail: *drjoshivarsha@gmail.com*).

See also the article by Phillips et al (pp 699–700) in this issue.

Teaching Point

Introduction

Congenital sensorineural hearing loss arises as a result of abnormalities in the inner ear, the vestibulocochlear nerve, or the processing centers of the brain. The abnormality may have a genetic cause or be a sequela of infection or injury at birth; in some cases, no cause is identified (1).

High-resolution computed tomography (CT) and magnetic resonance (MR) imaging of the temporal bones allow excellent depiction of inner ear malformations and are routinely used in the evaluation of pediatric sensorineural hearing loss. CT has always been the preferred imaging modality to delineate the intricate osseous anatomy and malformations of the inner ear, but high-resolution MR imaging is used with increasing frequency to study the membranous labyrinth and eighth cranial nerve (vestibulocochlear nerve) (2–5). An MR imaging examination of the brain, if performed at the same time as the inner ear examination, offers the advantage of allowing the evaluation of any coexistent brain parenchymal abnormalities (5). Preoperative high-resolution CT of the temporal bone allows the additional identification of middle and external ear abnormalities and provides anatomic information that is important for surgical planning. Together, these modalities play a vital role in the preoperative work-up for cochlear implantation.

For optimal interpretation of high-resolution CT and MR images obtained in children with congenital sensorineural hearing loss, the radiologist must have a comprehensive knowledge of the embryologic development of normal inner ear structures as well as the spectrum of malformations that may be encountered. Numerous classification systems have been proposed, none of which is all-inclusive. A fair amount of debate exists in regard to the definitions, terms, and stage of embryologic arrest (6,7).

The article describes standard imaging protocols used to evaluate the inner ear and illustrates the imaging features of various inner ear malformations in children with congenital sensorineural hearing loss. The malformations are described by using standard nomenclature and two widely accepted classification systems used by otolaryngologists for ease of interpretation (8,9). The impact of the identification of these malformations on prognosis and clinical management is discussed. A brief description of the relevant normal anatomy and development of the inner ear is provided. Brain abnormalities commonly seen in children with inner ear malformations are also discussed.

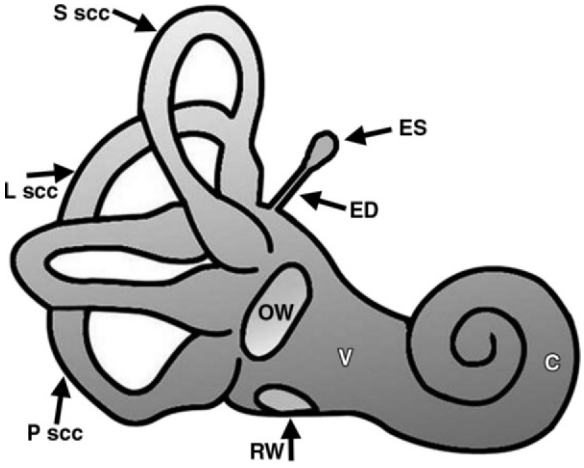

Figure 1. Drawing shows the normal anatomy of the inner ear: the cochlea *(C)*; vestibule *(V)*; superior semicircular canal *(Sscc)*; posterior semicircular canal *(Pscc)*; lateral semicircular canal *(Lscc)*; and vestibular aqueduct, which consists of an endolymphatic duct *(ED)* and endolymphatic sac *(ES)*. Note the locations of the oval window *(OW)* and round window *(RW)*.

Imaging Protocols

CT Examinations

High-resolution CT of the temporal bone, followed by image reconstruction in both the axial and coronal planes, is required to evaluate the inner ear and its malformations. Axial scanning is performed in planes parallel to the infraorbitomeatal line. On a multidetector CT scanner, the raw axial image data set can be reconstructed with a section thickness of as little as 0.3 mm to obtain high-quality coronal reformatted images. A 512 × 512 matrix is used, and all the images are reviewed with a high-resolution bone algorithm and a small field of view (9 cm) for separate documentation of the right and left ears. Axial images are obtained from the top of the petrous apex to the inferior tip of the mastoid bone. Coronal reformatted images are obtained from the anterior margin of the petrous apex to the posterior margin of the mastoid.

MR Imaging Examinations

The use of a 1.5- or 3-T MR imaging system is preferred for inner ear examinations, and sedation is used in most children. A thin-section gradient-echo sequence that is heavily T2 weighted is best suited for evaluation of the fluid-filled spaces of the membranous labyrinth and the eighth cranial nerve. A section thickness of as little as 0.4–0.7 mm is preferred for optimal delineation and to allow the generation of high-quality multiplanar reformatted images. A small

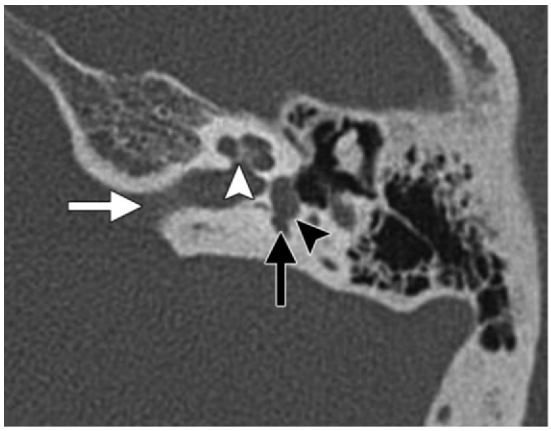

a.

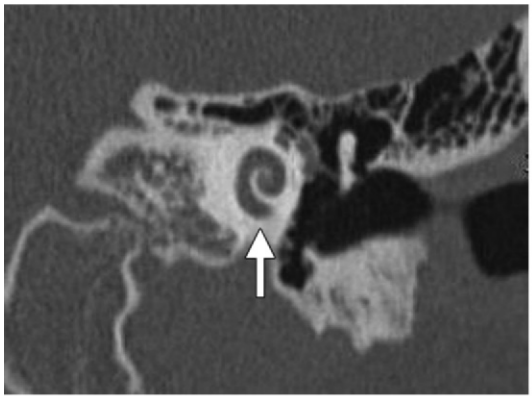

b.

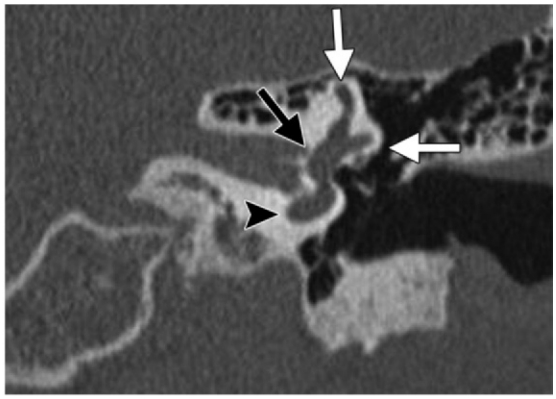

c.

Figure 2. High-resolution CT appearances of normal inner ear structures. **(a)** Axial image shows the modiolus within the cochlea (white arrowhead), the IAC (white arrow), the vestibule (black arrowhead), and the posterior semicircular canal (black arrow). **(b)** Coronal image shows the cochlea (arrow). **(c)** Coronal image obtained in a section slightly posterior to **b** shows the superior and lateral semicircular canals (white arrows). Black arrow = vestibule, arrowhead = basal turn of the cochlea.

field of view is used, and a volumetric acquisition is performed in the axial plane with sagittal and coronal reformatting. Oblique sagittal reformatted images are obtained in planes perpendicular to the course of the seventh and eighth nerves in the internal auditory canal (IAC) and cerebellopontine angle. Routine axial T2-weighted imaging of the brain should be performed in all patients to exclude central nervous system causes of sensorineural hearing loss (5).

Normal Anatomy of the Inner Ear

The anatomy of the temporal bone has been well described elsewhere in the literature (10,11). A few important features of the inner ear are described here.

The inner ear consists of an osseous labyrinth that encloses a membranous labyrinth. The osseous labyrinth consists of the vestibule, cochlea, semicircular canals, vestibular aqueduct, and cochlear aqueduct (Fig 1). The space between the osseous labyrinth and membranous labyrinth is filled with a fluid known as perilymph. A similar fluid (endolymph) fills the space within the membranous labyrinth.

The vestibule is the central, rounded portion of the osseous labyrinth. It is continuous anteroinferiorly with the cochlea and posteriorly with the semicircular canals and the vestibular aqueduct. The vestibule contains the utricle and the saccule, which are integral components of the membranous labyrinth. The vestibular aqueduct is a tubular structure that arises from the vestibule and runs along the posteroinferior aspect of the petrous temporal bone. It contains the endolymphatic duct and sac, which are connected to the utricle and saccule of the vestibule. The vestibular aqueduct is diagonally oriented in relation to the direction of the IAC. The aqueduct, which normally measures less than 1.5 mm in diameter, approximates the size of the posterior semicircular canal, which runs anterior and parallel to the aqueduct.

There are three semicircular canals; these are designated as the superior, lateral, and posterior semicircular canals (Figs 1, 2a, 2c). The posterior end of the superior semicircular canal joins the upper end of the posterior semicircular canal to form a common limb known as the common crus.

Figure 3. High-resolution MR images obtained with heavy T2 weighting show the fluid-filled spaces of the inner ear and the seventh and eighth cranial nerves. **(a)** Axial image shows the basal turn of the cochlea with the osseous spiral lamina (arrow). **(b)** Axial image shows the middle and apical turns with the modiolus (arrowhead) and the spiral lamina (curved arrow) dividing the cochlea into the scala vestibuli *(sv)* and the scala tympani *(st)*. The nerves are seen in the cerebellopontine angle and IAC (straight arrow). **(c)** Sagittal image shows the four nerves within the IAC: the facial nerve (straight arrow), cochlear nerve (curved arrow), and superior and inferior vestibular nerves (arrowheads).

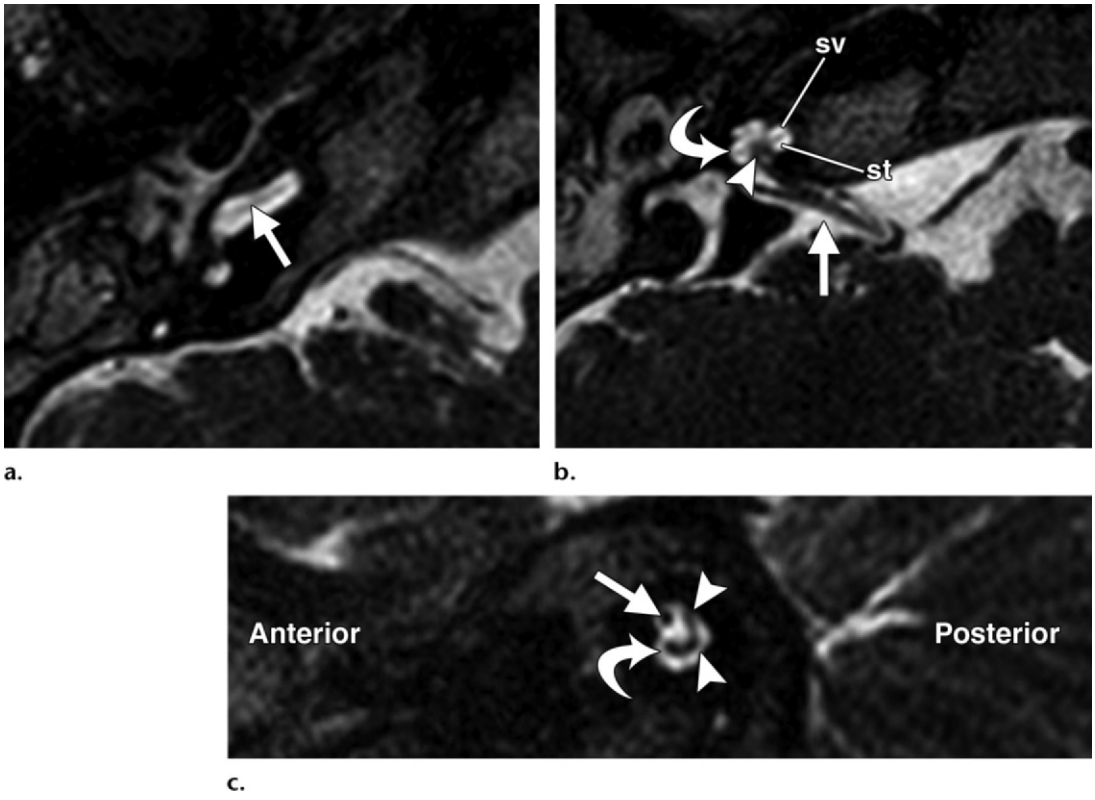

The cochlea (Figs 2, 3a, 3b) consists of a canal that spirals 2½ to 2¾ times around a central column of bone (the modiolus). The diameter of the canal decreases gradually as it proceeds toward the cochlear apex. A delicate osseous spiral lamina that projects from the modiolus divides the cochlear canal into an upper compartment (scala vestibuli) and a lower compartment (scala tympani). These two compartments communicate through an opening called the helicotrema, at the cochlear apex. The cochlear aqueduct is a thin osseous canal just inferior to the IAC and roughly parallel to it. The cochlear aperture, also known as the cochlear nerve canal, is a small opening at the fundus of the IAC through which the cochlear nerve enters the cochlea.

The IAC (Fig 2a) is separated from the vestibule by the lamina cribrosa. The IAC extends from the labyrinth to the cerebellopontine angle and contains the seventh and eighth cranial nerves (Fig 3b). The eighth nerve (vestibulocochlear nerve) is composed of three branches: The superior and inferior vestibular branches of the nerve occupy the posterosuperior and posteroinferior quadrants of the IAC, respectively; the cochlear branch is located in the anteroinferior quadrant. A normal cochlear branch of the eighth nerve should have approximately the same diameter as the facial nerve, which occupies the anterosuperior part of the IAC (Fig 3c).

Development of the Inner Ear

The inner ear arises from the otic placode in a process that begins early in the 3rd week of gestation. By the 8th week, the development of the cochlea is complete. The vestibule is completely developed by the 11th week, and the semicircular canals, between the 19th and 22nd weeks; the lateral canal or duct is the last to form. Ossification of the labyrinth is complete by the

Origin and Characteristics of Congenital Malformations of the Inner Ear

Type of Malformation	Gestational Week of Origin*	Manifestations	Percentage of Patients Affected†
Complete labyrinthine aplasia	3rd	Complete absence of inner ear structures	1
Cochlear aplasia	Late 3rd	Absent cochlea with normal or deformed vestibule and semicircular canals	3
Common cavity	4th	Confluent cochlea and vestibule forming a cystic cavity with no internal architecture; normal or deformed semicircular canals	25
Type I incomplete partition	5th	Cystic cochleovestibular malformation with absence of modiolus; cystic vestibule present but separated from cochlea; figure-eight or snowman-like appearance on axial CT and MR images	6
Cochlear hypoplasia	6th	Small cochlear bud with less than one turn; normal or deformed vestibule and semicircular canals	15
Type II incomplete partition	7th	Cochlea with normal basal turn and cystic apex; strong association with enlarged vestibular aqueduct	50

*Malformations are listed in progression from the least to the most differentiated.
†Numbers indicate the percentage of all patients with congenital inner ear malformations in whom the particular type of malformation is found.

23rd week, and the development of the inner ear is complete by the 26th week. Various inner ear malformations may result from developmental arrest at any prior stage, with the type of malformation depending on the gestational age at which the arrest occurs (8).

Inner Ear Malformations

Congenital malformations of the inner ear may be considered in two broad categories (12): *(a)* malformations with pathologic changes that involve only the membranous labyrinth and *(b)* malformations that involve both the osseous and the membranous labyrinth (malformed otic capsules).

Malformations of the Membranous Labyrinth

Several types of membranous labyrinth malformation have been described (12). These include complete membranous labyrinth dysplasia (Bing-Siebenmann malformation), cochleosaccular dysplasia (Scheibe malformation), and cochlear basal turn dysplasia (Alexander dysplasia). The classification of these abnormalities is not clinically useful, as their differentiation requires histopathologic examination.

Malformations of Both the Osseous and the Membranous Labyrinth

Teaching Point

Various deformities that involve both the osseous and the membranous labyrinth have been described. Most such deformities are linked to the gestational age at which the developmental failure or insult occurred (Table). The identification of this type of malformation at radiologic imaging heavily influences both the clinical management strategy and the prognosis (13). Many syndromes with associated inner ear malformations have been described elsewhere; the following discussion focuses on specific types of inner ear malformation, drawing on the classification systems developed by Jackler et al (8) and Sennaroglu and Saatci (9).

Complete Labyrinthine Aplasia.—Complete labyrinthine aplasia, also known as Michel aplasia (because it was first described by Michel in 1863), is the most severe form of inner ear deformity; it is caused by developmental arrest of the otic placode during the 3rd gestational week (7–9,12,14,15). The condition is extremely rare, accounting for only 1% of all inner ear malformations (14).

Figure 4. Complete labyrinthine aplasia. **(a)** Axial high-resolution CT image shows the absence of inner ear structures. Note the flat medial wall of the middle ear cavity (arrow) and the hypoplastic petrous bone (*). **(b)** Coronal CT image shows an atretic IAC (arrow). **(c)** Sagittal MR image obtained in a plane perpendicular to the IAC depicts a single nerve (arrow) within the small IAC. Combined with the findings in **a** and **b**, this feature is suggestive of absence of the eighth cranial nerve.

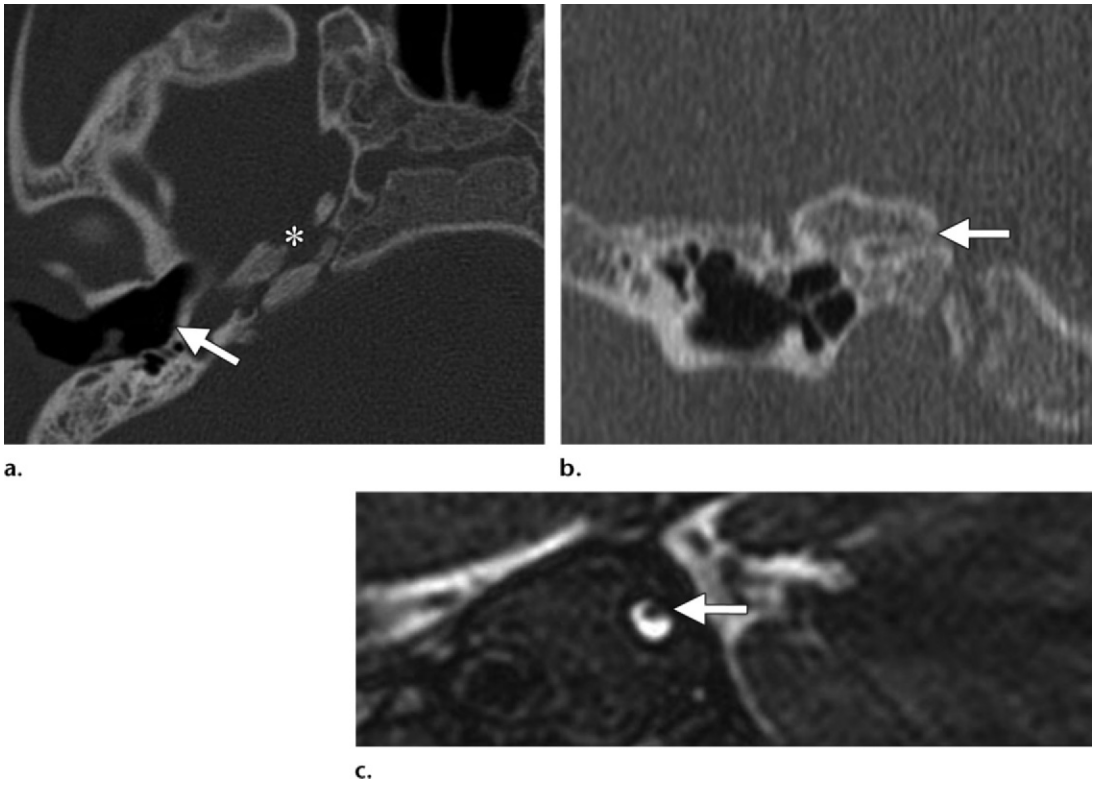

Complete labyrinthine aplasia is defined by the complete absence of inner ear structures (Fig 4a). A narrow, atretic IAC is seen on high-resolution CT images (Fig 4b), and the eighth cranial nerve is not visualized on MR images (Fig 4c). These abnormalities may be unilateral or bilateral (14,15). In patients with unilateral complete labyrinthine aplasia, the contralateral inner ear structures are often dysplastic.

Multiple associated abnormalities have been described in structures arising from the otic capsule (14,15). Hypoplasia of the petrous bone, absence of the round and oval windows, and flattening of the medial wall of the middle ear cavity (Fig 4a) are characteristic features. Dysplastic stapes and varying degrees of hypoplasia of the middle ear cavity and mastoid bone may be seen. Labyrinthine aplasia also may be associated with skull base and vascular anomalies, such as platybasia, abnormal courses of the transverse sinus and jugular veins, and craniocervical junction anomalies. Anomalous courses of the facial nerve also have been described. Posterior fossa abnormalities, such as arachnoid cysts, may be seen. Sclerotic deposits often are found in the hypoplastic petrous bone, although they are nonspecific to aplasia and may be seen also in labyrinthitis ossificans. A flat appearance of the medial wall of the middle ear, a characteristic finding of complete labyrinthine aplasia, helps better differentiate it from labyrinthitis ossificans (14,15).

Cochlear Aplasia.—Cochlear aplasia, or complete absence of the cochlea, is most likely due to arrested development of the inner ear in the latter part of the 3rd week of gestation (7) or, as described by some, in the 5th week (6). It is a rare anomaly, accounting for only 3% of cochlear

Figures 5, 6. Differentiation of cochlear aplasia from labyrinthitis ossificans. **(5)** Cochlear aplasia. **(a)** Drawing shows absence of the cochlea, dilatation of the vestibule *(v)*, and deformity of the lateral semicircular canal *(scc)*, characteristics of cochlear aplasia. **(b)** Axial CT image shows a dilated globose vestibule (arrowhead), dense bone where the cochlea should be (curved arrow), and a stunted, dilated posterior semicircular canal (straight arrow). **(c)** Coronal CT image shows a malformed, dilated lateral semicircular canal (straight arrow) with a stunted superior semicircular canal (curved arrow). **(6)** Labyrinthitis ossificans. Coronal CT image obtained in another patient shows abnormal bone deposition in the cochlea (straight arrow) anterior to the IAC, with a normal cochlear promontory (curved arrow) produced by the basal turn of the cochlea. These features are seen in labyrinthitis ossificans but not in cochlear aplasia.

5a.

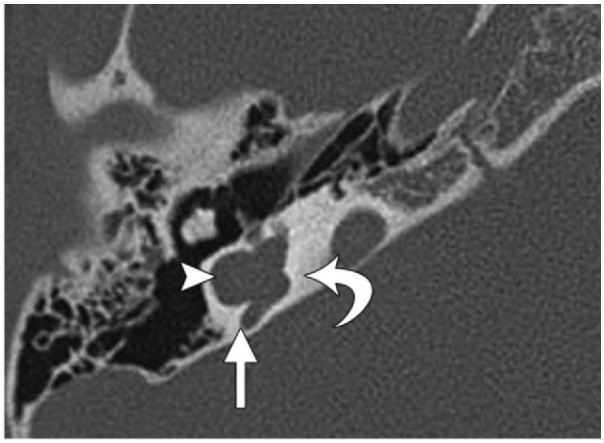

5b.

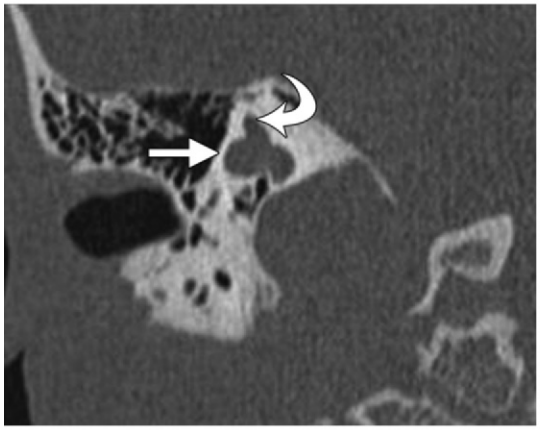

5c.

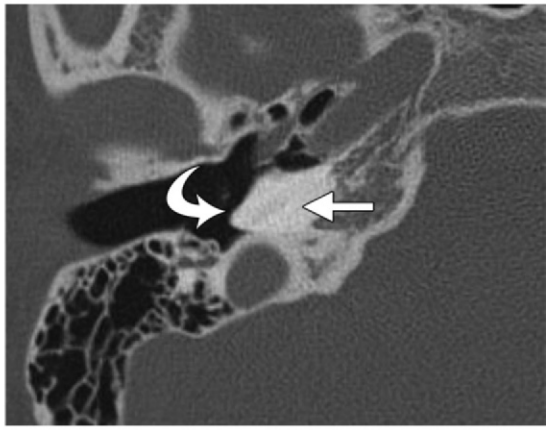

6.

malformations. In cochlear aplasia, the vestibule and semicircular canals are often malformed but may be normal (5,7–9,12). Dense otic bone is present at the site where the cochlea normally would be and is best depicted on CT images. It is important to differentiate this anomaly from labyrinthitis ossificans, in which normal-sized bone is seen anterior to the IAC, with the bulge of the cochlear promontory produced by the basal turn of the cochlea; both features are absent in cochlear aplasia (Figs 5, 6).

Common Cavity.—A common cavity results from a developmental arrest in the 4th week of gestation and accounts for about 25% of all cochlear malformations (5,12). This malformation is defined by the absence of the normal differentiation between the cochlea and vestibule (Fig 7a). CT and MR images show confluence of the cochlea and vestibule in a cystic cavity with no internal

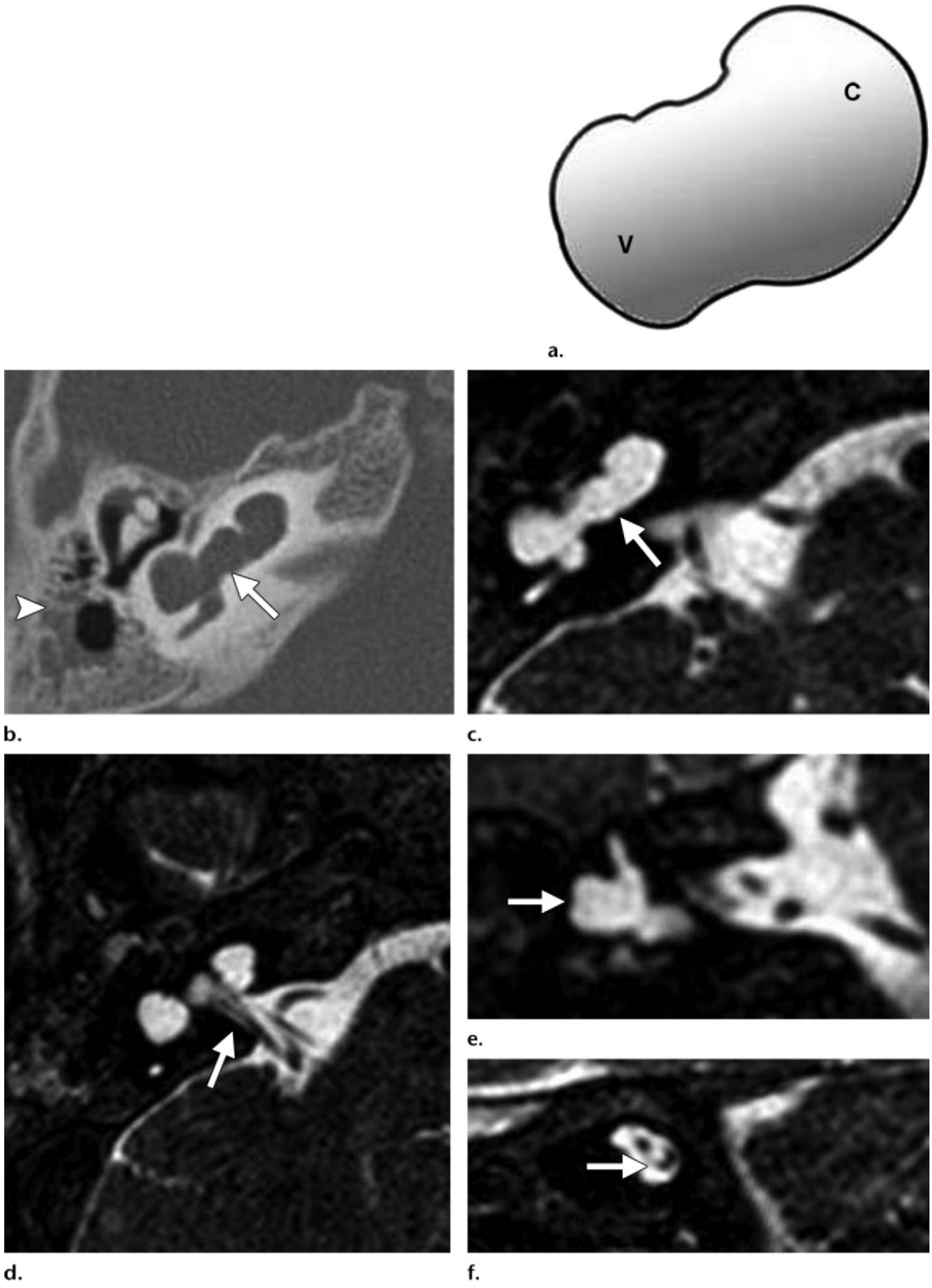

Figure 7. Common cavity. **(a)** Drawing shows a common cavity formed by the vestibule *(v)* and the cochlea *(c)*. **(b)** Axial CT image shows confluence of the cochlea and vestibule in a cystic cavity with no internal architecture (straight arrow). An effusion (arrowhead) is seen in the mastoid air cells. **(c–e)** Axial T2-weighted gradient-echo MR images show the common cavity (arrow in **c**), a dilated IAC (arrow in **d**), and a malformed lateral semicircular canal (arrow in **e**). **(f)** Sagittal MR image shows absence of the cochlear nerve (arrow).

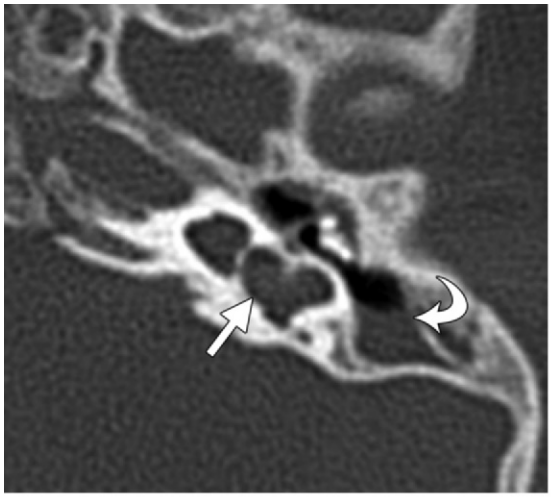

a.

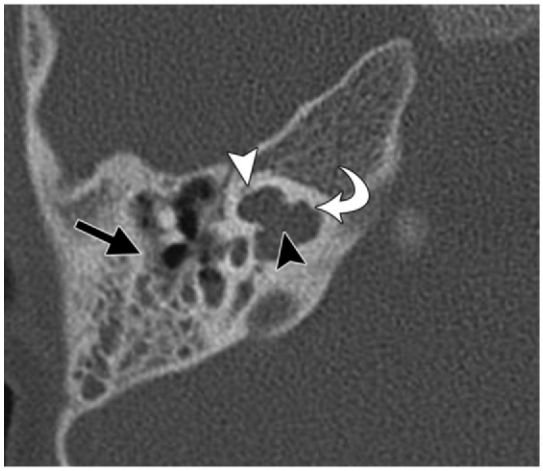

b.

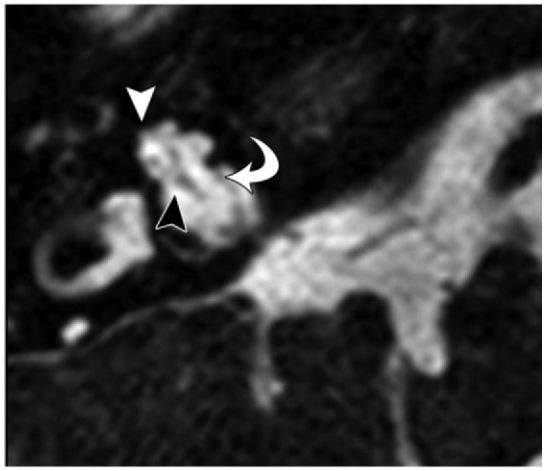

c.

Figure 8. Type I incomplete partition. **(a)** Axial CT image shows a cystic cochlea without any internal architecture, accompanied by a dilated vestibule that forms a figure eight (straight arrow). Note the coexistent mucosal disease in the mastoid air cells and middle ear (curved arrow). **(b, c)** Axial CT **(b)** and MR **(c)** images obtained in another patient show a cystic cochlea (white arrowhead) that is separated from a dilated IAC (curved arrow) by a partially dehiscent cribriform plate (black arrowhead). Straight arrow in **b** = opacification of the middle ear and mastoid air cells.

architecture (Fig 7b, 7c). The width of the cavity is typically greater than its height, with the average vertical diameter being 7 mm, and the average horizontal diameter, 10 mm (11,12). The semicircular canals are frequently malformed but occasionally normal (Fig 7e).

Type I Incomplete Partition.—Type I incomplete partition is also known as cystic cochleovestibular malformation (9). It most likely results from a developmental arrest in the 5th week of gestation (7). The modiolus is entirely absent; the cochlea has a cystic appearance; and the vestibule is often dilated, forming a figure eight (7) (Fig 8a). The fact that the vestibule is distinguishable from the cochlea makes it possible to differentiate a type I incomplete partition from a common cavity. The vestibular aqueduct is normal. The cribriform area between the cochlea and IAC is often defective, and all patients have a large IAC (Fig 8b, 8c), predisposing them to increased risks for meningitis and for a perilymphatic gusher in the event of surgery (7). Type I incomplete partition is less well differentiated than type II incomplete partition.

Cochlear Hypoplasia.—Cochlear hypoplasia results from an aberration in the development of the cochlear duct during the 6th week of gestation (5,7,12). This abnormality accounts for 15% of cochlear malformations. At CT and MR imaging, a small cochlear bud of variable length (usually 1–3 mm) is seen protruding from the vestibule (Fig 9a–9c), and an abnormally small IAC may be seen (Fig 9d). Although the cochlea is visible, it has only one turn or a partial turn (Fig 9e). The vestibule and semicircular canals are usually malformed but may be normal (Fig 9f) (7–9,12).

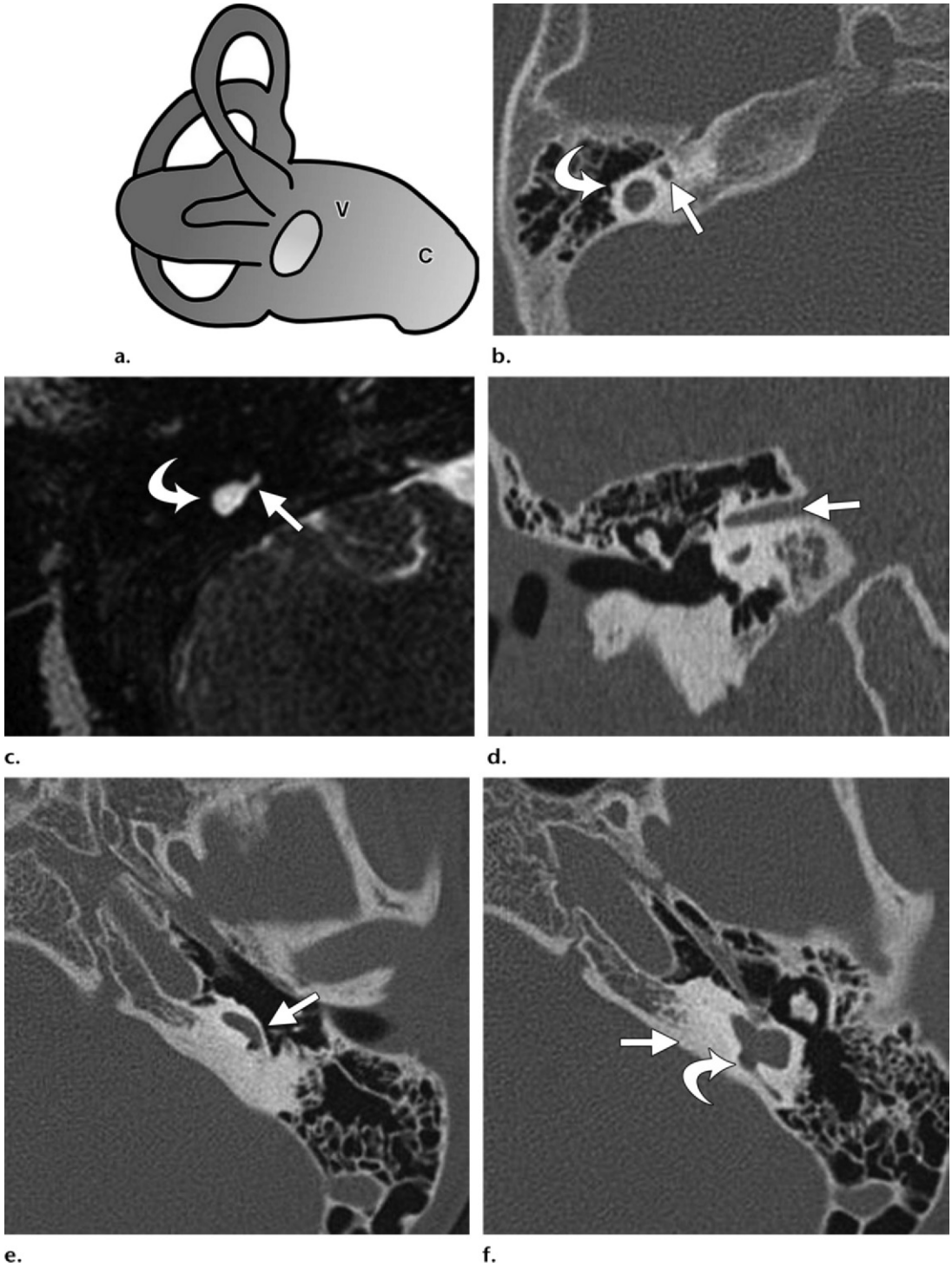

Figure 9. Cochlear hypoplasia. **(a)** Drawing shows a small cochlear bud *(c)* and an abnormally small, deformed vestibule *(v)*. **(b–d)** In a patient with cochlear hypoplasia, axial CT **(b)** and MR **(c)** images depict a small cochlear bud (curved arrow) and small vestibule (straight arrow), and coronal CT image **(d)** shows a stenotic IAC (arrow). **(e, f)** Axial CT images obtained in another patient show a cochlea with only a basal turn (arrow in **e**); the rest of the cochlea is undeveloped. Sclerotic bone (straight arrow in **f**) is seen in the region of the cochlea, with an abnormal, dilated vestibule (curved arrow in **f**).

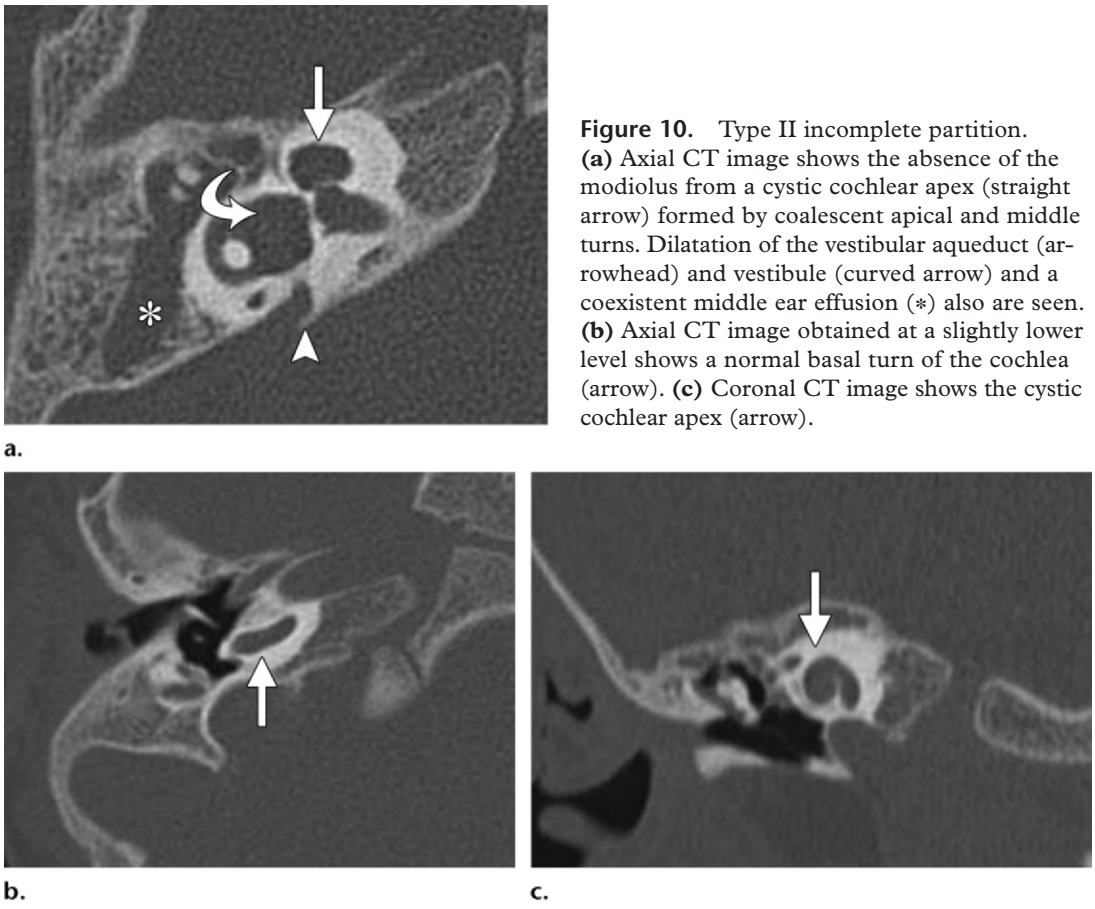

Figure 10. Type II incomplete partition. **(a)** Axial CT image shows the absence of the modiolus from a cystic cochlear apex (straight arrow) formed by coalescent apical and middle turns. Dilatation of the vestibular aqueduct (arrowhead) and vestibule (curved arrow) and a coexistent middle ear effusion (*) also are seen. **(b)** Axial CT image obtained at a slightly lower level shows a normal basal turn of the cochlea (arrow). **(c)** Coronal CT image shows the cystic cochlear apex (arrow).

Type II Incomplete Partition.—Type II incomplete partitition (Mondini deformity) represents a developmental arrest in the 7th week of gestation (7,12). It is the most common type of cochlear malformation, accounting for more than 50% of all cochlear deformities (12). In type II incomplete partition, the cochlea consists of 1½ turns, and the interscalar septum and osseous spiral lamina are absent. The basal cochlear turn appears normal, but the middle and apical turns coalesce to form a cystic apex. The modiolus is present only at the level of the basal turn. Type II incomplete partition is often associated with a large endolymphatic duct and sac and an enlarged vestibular aqueduct (9,12). The association of these features is so strong that this type of malformation has been described as a triad consisting of a cochlea with a normal basal turn and cystic apex, enlarged vestibular aqueduct and vestibule, and normal semicircular canals (7) (Fig 10). At MR imaging, where one normally expects to see distinct scalae tympani and vestibuli, the interscalar septal defects and the absence of the osseous spiral lamina from the middle and apical turns are easily distinguished on thin-section gradient-echo images obtained with heavy T2 weighting.

Malformations of the Vestibule and Semicircular Canals.—The development of the semicircular canals begins between the 6th and 8th weeks of gestation and is completed between the 19th and 22nd weeks (5,10). The superior semicircular canal develops first, and the lateral semicircular canal develops last. Hence, malformation of the superior and posterior semicircular canals without involvement of the lateral canal is unusual. The malformed canals are usually short and wide but may be narrow. In extensive malformations, the vestibule is dilated and forms a common lumen with the lateral canal (Fig 11a, 11b). This type of abnormality, which has been described as "lateral semicircular canal–vestibule dysplasia," may be accompanied by a normal or malformed cochlea, depending on the stage of inner ear development at the time of embryologic arrest (5,10).

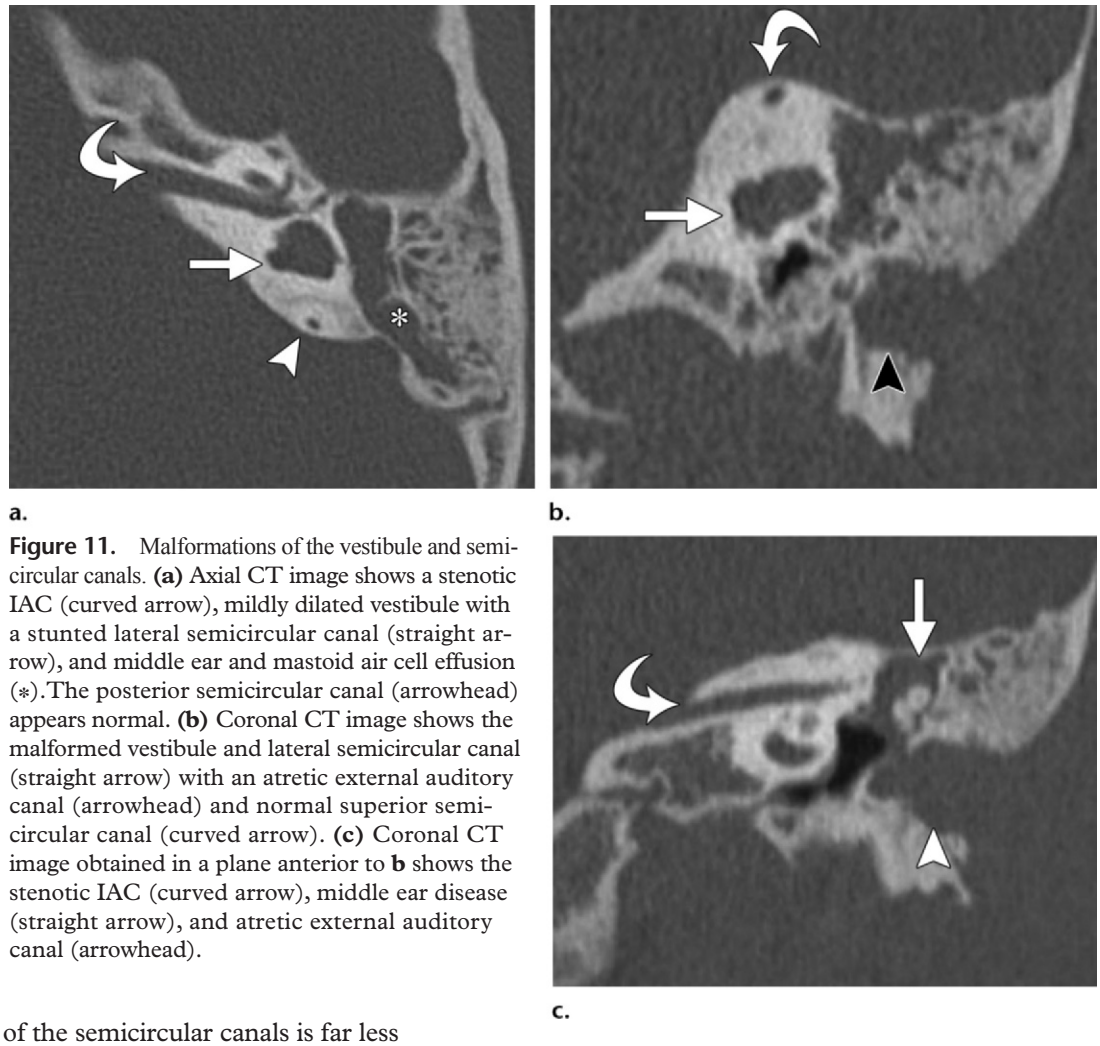

Figure 11. Malformations of the vestibule and semicircular canals. **(a)** Axial CT image shows a stenotic IAC (curved arrow), mildly dilated vestibule with a stunted lateral semicircular canal (straight arrow), and middle ear and mastoid air cell effusion (*).The posterior semicircular canal (arrowhead) appears normal. **(b)** Coronal CT image shows the malformed vestibule and lateral semicircular canal (straight arrow) with an atretic external auditory canal (arrowhead) and normal superior semicircular canal (curved arrow). **(c)** Coronal CT image obtained in a plane anterior to **b** shows the stenotic IAC (curved arrow), middle ear disease (straight arrow), and atretic external auditory canal (arrowhead).

Aplasia of the semicircular canals is far less common than dysplasia. In this condition, too, the cochlea may be normal or deformed. An abnormal course of the facial nerve, atresia of the oval window, and abnormal ossicles are frequently seen in children with aplasia of the canals (16). Absence of all semicircular ducts is known to occur frequently in patients with CHARGE syndrome (a combination of coloboma, heart anomalies, choanal atresia, retardation of growth and development, and genital and ear anomalies) (16,17). Isolated aplasia of the posterior semicircular duct has been described in patients with Waardenburg syndrome and Alagille syndrome (16).

Teaching Point

It is essential to perform high-resolution CT to confirm the diagnosis of semicircular canal aplasia. Aplasia and fibrous or calcified obliteration of the canals have the same appearance at MR imaging. However, at CT, the semicircular canal is absent in cases of aplasia, whereas a normal canal is seen in cases of fibrous obliteration (since fibrous tissue cannot be seen at CT) and calcifications within the canal are seen in cases of labyrinthitis ossificans (5).

Vestibular malformations rarely occur in isolation. Commonly encountered anomalies include mild or globose dilatation of the vestibule with partial or complete assimilation of the semicircular canals into the vestibule (5,7).

Measurement of the width of the central bony islands of the superior and lateral semicircular canals on axial high-resolution CT images has been proposed as a means for identifying any subtle abnormalities of the semicircular canals that may exist in children with congenital sensorineural hearing loss whose inner ear anatomy appears normal on CT and MR images (18,19).

Enlarged Vestibular Aqueduct.—An enlarged vestibular aqueduct, or an enlarged endolymphatic duct and sac, is the most frequent CT or MR imaging finding in patients with early-onset sensorineural hearing loss and was the most frequent inner ear malformation reported in some recent studies (20). The abnormality is bilateral in as many as 90% of cases, may be asymmetric, and is slightly more common in females. Al-

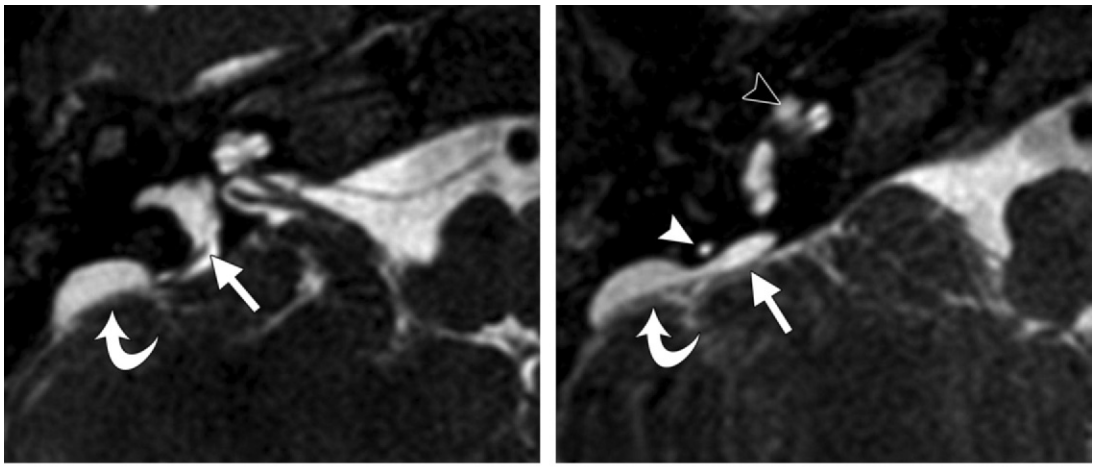

a. b.

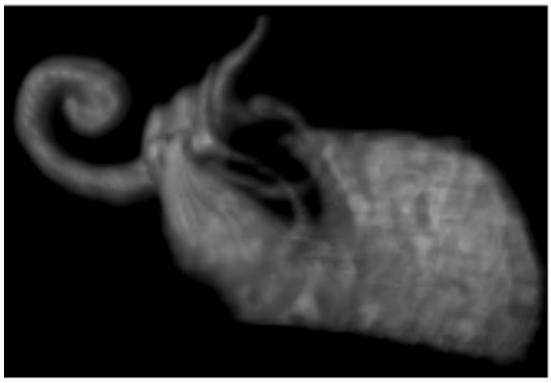

c.

Figure 12. Enlarged vestibular aqueduct. **(a, b)** Axial MR images show marked dilatation of the endolymphatic duct (straight arrow) and sac (curved arrow) in comparison with the normal posterior semicircular canal (white arrowhead in **b**). The modiolus is not seen in the middle and apical turns of the cochlea (black arrowhead in **b**). **(c)** Three-dimensional image reconstructed from the same image dataset as in **a** and **b** shows the dilated endolymphatic duct and sac.

though enlargement of the vestibular aqueduct most likely is the result of a developmental anomaly in the 7th week of gestation, the vestibular aqueduct continues to develop throughout gestation and beyond; thus, in some cases, the malformation may actually be acquired and not congenital (7). Those affected typically experience a sudden onset of hearing loss that fluctuates in severity and that may be aggravated by minor head trauma, barometric pressure changes, or activity that causes increased intracranial pressure.

The characteristic imaging feature seen at CT is enlargement of the osseous vestibular aqueduct. At MR imaging, the characteristic feature is enlargement of the endolymphatic duct and sac (5). The vestibular aqueduct is considered enlarged when its diameter midway between the common crus and the external aperture is greater than 1.5 mm on CT images (Fig 10a). The fluid-containing posterior semicircular duct also has a diameter of approximately 1.5 mm, and its ascending portion is situated anterior and parallel to the endolymphatic duct and sac. The endolymphatic duct and sac may be considered enlarged when their diameters exceed that of the adjacent ascending portion of the posterior semicircular duct on thin-section T2-weighted gradient-echo images (Fig 12a, 12b).

In 84% of cases, an enlarged vestibular aqueduct is accompanied by other inner ear anomalies, and an isolated finding of enlargement of the endolymphatic duct and sac is uncommon (20). Cochlear anomalies are present in most cases of endolymphatic duct and sac enlargement and range from subtle modiolar deficiency (Fig 12a) and scalar asymmetry to gross dysplasia. An enlarged vestibular aqueduct and associated cochlear abnormalities are best assessed on axial thin-section high-resolution T2-weighted gradient-echo images. Replacement of the normally high-signal-intensity fluid inside the dilated endolymphatic duct and sac by low-signal-intensity material is often seen, most frequently in the posterior part of the duct, near the sigmoid sinus, because of the presence there of loose connective and fibrous tissue. Enlargement of the vestibular aqueduct may be accompanied by dysplasia of one or more of the semicircular canals as well as by enlargement of the vestibule. An enlarged vestibular aqueduct is frequently seen in Pendred syndrome, which is characterized by congenital sensorineural hearing loss and goiter.

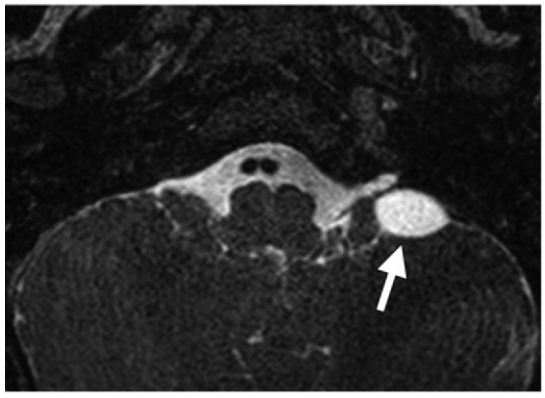

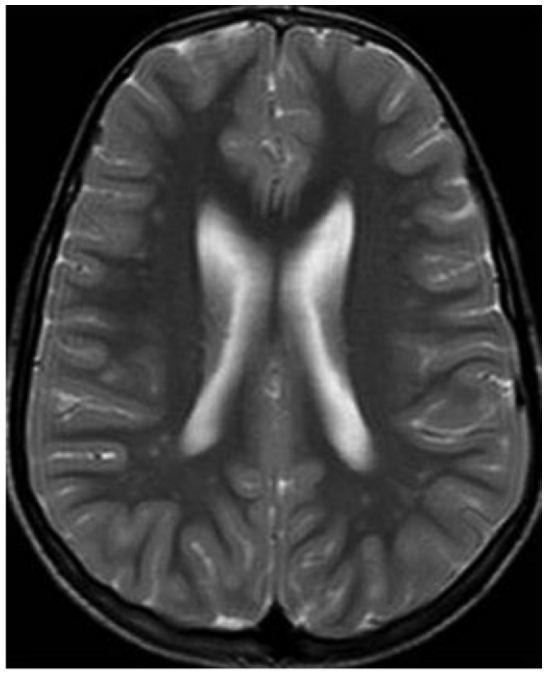

a. b.

Figure 13. Brain abnormalities. **(a)** Axial T2-weighted MR image obtained in a child with complete labyrinthine aplasia shows an arachnoid cyst (arrow). **(b)** Axial T2-weighted MR image obtained in another child with congenital sensorineural hearing loss shows focal white-matter signal abnormalities.

Coexistent cochlear anomalies have important implications for therapeutic planning and prognosis. Successful cochlear implantation depends on the integrity of the underlying cochlea (21). In children with bilateral enlargement of the vestibular aqueduct, the imaging findings can help the surgeon determine which ear has the more normal anatomy and thus influence decision making for surgical implantation.

IAC and Cochlear Nerve Anomalies.—The normal diameter of the IAC ranges from 2 to 8 mm, with an average of 4 mm. An IAC with a diameter of less than 2 mm is described as stenotic (6,22). The IAC may also be atretic or may have a bony septum that partitions it into two or more separate canals. The morphologic characteristics and size of the IAC are not reliable indicators of the integrity of the cochlear nerve, and normal size of the IAC and normal inner ear anatomy do not exclude a nerve deficiency; the nerve may even be absent when the IAC and labyrinth are completely normal. Hence, high-resolution MR imaging is the preferred modality for accurate assessment of the cochlear nerve (23).

Teaching Point

Sagittal oblique images obtained in a plane perpendicular to the long axis of the IAC provide the best depiction of the four major nerves of the IAC: the facial, cochlear, superior vestibular, and inferior vestibular nerves (24). Three types of cochlear nerve anomalies have been described (24). In a type 1 cochlear nerve anomaly, a stenotic IAC is seen with an absent eighth nerve (Fig 4b, 4c). In a type 2 anomaly, a common vestibulocochlear nerve is found, with hypoplasia or aplasia of its cochlear branch. When this anomaly is associated with other inner ear malformations, it is referred to as a type 2A malformation (Fig 7f). When the anomaly occurs in isolation (ie, the inner ear is normal in other respects), it is referred to as a type 2B malformation.

The cochlear aperture is a small canal at the fundus of the IAC through which the cochlear nerve passes to enter the cochlea (24). When the site of the cochlear aperture is filled by bone, the condition is described as hypoplasia of the bony canal of the cochlear nerve (25).

Brain Abnormalities.—An increased incidence of posterior fossa abnormalities such as asymmetric dilatation of the fourth ventricle and arachnoid cysts (Fig 13a) has been observed among patients with complete labyrinthine aplasia (14). Neuronal migration abnormalities in children with congenital sensorineural hearing loss also have been described (26). Congenital cytomegalovirus infection contributes substantially to sensorineu-

Teaching Point

RadioGraphics

ral hearing loss in many infant populations. The discrete foci of white-matter signal abnormality that are frequently seen on MR images obtained in children with sensorineural hearing loss (Fig 13b) have been attributed to cytomegalovirus infection at birth (27,28).

Implications of Imaging Abnormalities for Cochlear Implantation

Congenital inner ear malformations have been classified by Ramos et al (13) into three groups with respect to their implications for the feasibility of cochlear implantation surgery: *(a)* gross malformations constituting surgical contraindications, *(b)* major malformations contributing to increased risks for complications, and *(c)* minor malformations.

Gross malformations such as complete labyrinthine aplasia, cochlear aplasia, and cochlear nerve deficiency are contraindications for cochlear implantation surgery. Patients in whom the cochlear nerve is not seen on MR images—whether because the nerve is too slender to discern or because its fibers parallel those of the vestibular nerve and are inseparable from it—may not do well after cochlear implantation and should undergo evaluation by an experienced audiologist before the decision about implantation is made (28–30).

In the presence of a major malformation (eg, a common cavity or severe hypoplasia), the result of cochlear implantation is often difficult to predict. Severe malformations often are associated with higher intraoperative risks for cerebrospinal fluid leakage, postimplantation meningitis, and potential electrode displacement.

Minor malformations include partition defects such as hypoplasia, abnormalities of the aqueduct, and abnormalities of the vestibule. If bilateral malformations are found, the surgeon will want to know which inner ear has the more normal structure and the larger cochlear nerve. If the cochlear nerve is not clearly seen at preoperative imaging, it is recommended that intracochlear electrical stimulation be performed to determine the auditory nerve action potential and auditory brainstem response before cochlear implantation is undertaken (13,30).

High-resolution CT provides useful information not only about inner ear malformations but also about the presence of other anatomic variants and the status of the external and middle ear, which might affect surgical decision making. A few anatomic variants that are noteworthy when planning cochlear implantation surgery are an aberrant course of the carotid artery, a high-riding or dehiscent jugular bulb, an aberrant course of the facial nerve, and a dehiscent facial nerve canal. Effusions in the middle ear and mastoid air cells can readily be seen on high-resolution CT images and should be reported to the surgeon before cochlear implantation is undertaken. Surgeons also appreciate mention of the degree of mastoid pneumatization and middle ear development, features that are easily assessed at high-resolution CT.

Conclusions

Inner ear malformations are found in 15%–20% of patients with severe or profound sensorineural hearing loss. High-resolution CT and MR imaging play an important role in the evaluation of pediatric hearing loss by providing crucial information about the inner ear, vestibulocochlear nerve, and brain. Both modalities precisely and accurately delineate the inner ear anatomy and malformations. They are often complementary and are used together in the preoperative evaluation of pediatric candidates for cochlear implantation. Preoperative high-resolution CT offers the advantage of visualizing any coexistent middle or external ear anomalies and important anatomic variants, and MR imaging provides definitive information about the integrity of the cochlear nerve and the fluid-filled spaces of the inner ear. MR imaging is superior to CT for the identification of an enlarged vestibular aqueduct. The additional acquisition of axial T2-weighted MR images of the brain during imaging of the inner ear allows the identification of brain abnormalities that commonly coexist with congenital inner ear malformations. White-matter lesions frequently seen in these children are attributed to congenital cytomegalovirus infection.

A clear understanding of the embryogenesis and anatomy of the inner ear and the standard classification systems for describing inner ear malformations are fundamental to the interpretation of CT and MR images. Identification of the inner ear abnormality has a substantial effect on clinical decision making, prognosis, and management strategy.

Acknowledgment.—The authors thank Imron Subhan, MD, for his assistance with preparation of the figures.

References

1. Grundfast KM, Siparsky NF. Hearing loss. In: Bluestone CD, Stool SE, Alper CM, et al, eds. Pediatric otolaryngology. Vol 1. Philadelphia, Pa: Saunders, 2003; 306–350.

2. Parry DA, Booth T, Roland PS. Advantages of magnetic resonance imaging over computed tomography in preoperative evaluation of pediatric cochlear implant candidates. Otol Neurotol 2005;26(5):976–982.
3. Casselman JW, Kuhweide R, Ampe W, et al. Inner ear malformations in patients with sensorineural hearing loss: detection with gradient-echo (3DFT-CISS) MRI. Neuroradiology 1996;38(3):278–286.
4. Ellul S, Shelton C, Davidson HC, Harnsberger HR. Preoperative cochlear implant imaging: is magnetic resonance imaging enough? Am J Otol 2000;21(4):528–533.
5. Casselman JW, Offeciers EF, De Foer B, Govaerts P, Kuhweide R, Somers T. CT and MR imaging of congential abnormalities of the inner ear and internal auditory canal. Eur J Radiol 2001;40(2):94–104.
6. Romo LV, Casselman JW, Robson CD. Temporal bone: congenital anomalies. In: Som PM, Curtin HD, eds. Head and neck imaging. 4th ed. Vol 2. St Louis, Mo: Mosby, 2003; 1119–1140.
7. Swartz JD, Mukherji SK. The inner ear and otodystrophies. In: Swartz JD, Loevner LA, eds. Imaging of the temporal bone. 4th ed. New York, NY: Thieme, 2009; 298–411.
8. Jackler RK, Luxford WM, House WF. Congenital malformations of the inner ear: a classification based on embryogenesis. Laryngoscope 1987;97(3 Pt 2, Suppl 40):2–14.
9. Sennaroglu L, Saatci I. A new classification for cochleovestibular malformations. Laryngoscope 2002;112(12):2230–2241.
10. Curtin HD, Sanelli PC, Som PM. Temporal bone: embryology and anatomy. In: Som PM, Curtin HD, eds. Head and neck imaging. 4th ed. Vol 2. St Louis, Mo: Mosby, 2003; 1057–1075.
11. Donaldson JA, Duckert LG, Lambert PM, Rubel EW. Surgical anatomy of the temporal bone. 4th ed. New York, NY: Raven, 1992.
12. Jackler RK. Congenital malformations of the inner ear. In: Cummings CW, Flint PW, Harker LA, et al, eds. Cummings otolaryngology: head and neck surgery. 4th ed. Philadelphia, Pa: Elsevier Mosby, 2005; 4413–4414.
13. Ramos A, Cervera J, Valdivieso A, Pérez D, Vasallo JR, Cuyas JM. Cochlear implant in congenital malformations [in Spanish]. Acta Otorrinolaringol Esp 2005;56(8):343–348.
14. Ozgen B, Oguz KK, Atas A, Sennaroglu L. Complete labyrinthine aplasia: clinical and radiologic findings with review of the literature. AJNR Am J Neuroradiol 2009;30(4):774–780.
15. Marsot-Dupuch K, Dominguez-Brito A, Ghasli K, Chouard CH. CT and MR findings of Michel anomaly: inner ear aplasia. AJNR Am J Neuroradiol 1999;20(2):281–284.
16. Shin CH, Hong HS, Yi BH, et al. CT and MR imagings of semicircular canal aplasia. J Korean Soc Radiol 2009;61:9–15.
17. Morimoto AK, Wiggins RH 3rd, Hudgins PA, et al. Absent semicircular canals in CHARGE syndrome: radiologic spectrum of findings. AJNR Am J Neuroradiol 2006;27(8):1663–1671.
18. Purcell DD, Fischbein N, Lalwani AK. Identification of previously "undetectable" abnormalities of the bony labyrinth with CT measurement. Laryngoscope 2003;113(11):1908–1911.
19. Chen JL, Gittleman A, Barnes PD, Chang KW. Utility of temporal bone computed tomographic measurements in the evaluation of inner ear malformations. Arch Otolaryngol Head Neck Surg 2008;134(1):50–56.
20. Mafee MF, Charletta D, Kumar A, Belmont H. Large vestibular aqueduct and congenital sensorineural hearing loss. AJNR Am J Neuroradiol 1992;13(2):805–819.
21. Davidson HC, Harnsberger HR, Lemmerling MM, et al. MR evaluation of vestibulocochlear anomalies associated with large endolymphatic duct and sac. AJNR Am J Neuroradiol 1999;20(8):1435–1441.
22. Valvassori GE, Pierce RH. The normal internal auditory canal. Am J Roentgenol Radium Ther Nucl Med 1964;92:1232–1241.
23. Adunka OF, Roush PA, Teagle HFB, et al. Internal auditory canal morphology in children with cochlear nerve deficiency. Otol Neurotol 2006;27(6):793–801.
24. Glastonbury CM, Davidson HC, Harnsberger HR, Butler J, Kertesz TR, Shelton C. Imaging findings of cochlear nerve deficiency. AJNR Am J Neuroradiol 2002;23(4):635–643.
25. Fatterpekar GM, Mukherji SK, Alley J, Lin Y, Castillo M. Hypoplasia of the bony canal for the cochlear nerve in patients with congenital sensorineural hearing loss: initial observations. Radiology 2000;215(1):243–246.
26. Lapointe A, Viamonte C, Morriss MC, Manolidis S. Central nervous system findings by magnetic resonance in children with profound sensorineural hearing loss. Int J Pediatr Otorhinolaryngol 2006;70(5):863–868.
27. Haginoya K, Ohura T, Kon K, et al. Abnormal white matter lesions with sensorineural hearing loss caused by congenital cytomegalovirus infection: retrospective diagnosis by PCR using Guthrie cards. Brain Dev 2002;24(7):710–714.
28. Fowler KB, Boppana SB. Congenital cytomegalovirus (CMV) infection and hearing deficit. J Clin Virol 2006;35(2):226–231.
29. Warren FM 3rd, Wiggins RH 3rd, Pitt C, Harnsberger HR, Shelton C. Apparent cochlear nerve aplasia: to implant or not to implant? Otol Neurotol 2010;31(7):1088–1094.
30. Gupta SS, Maheshwari SR, Kirtane MV, Shrivastav N. Pictorial review of MRI/CT scan in congenital temporal bone anomalies, in patients for cochlear implant. Indian J Radiol Imaging 2009;19(2):99–106.

CT and MR Imaging of the Inner Ear and Brain in Children with Congenital Sensorineural Hearing Loss

Varsha M. Joshi, DNB • Shantanu K. Navlekar, DMRD • G. Ravi Kishore, MBBS • K. Jitender Reddy, MD • E. C. Vinay Kumar, MS

RadioGraphics 2012; 32:683–698 • **Published online** 10.1148/rg.323115073 • **Content Codes:** HN NR PD

Page 684
CT has always been the preferred imaging modality to delineate the intricate osseous anatomy and malformations of the inner ear, but high-resolution MR imaging is used with increasing frequency to study the membranous labyrinth and eighth cranial nerve (vestibulocochlear nerve) (2–5). An MR imaging examination of the brain, if performed at the same time as the inner ear examination, offers the advantage of allowing the evaluation of any coexistent brain parenchymal abnormalities (5). Preoperative high-resolution CT of the temporal bone allows the additional identification of middle and external ear abnormalities and provides anatomic information that is important for surgical planning.

Page 687 (Table on page 687)
Various deformities that involve both the osseous and the membranous labyrinth have been described. Most such deformities are linked to the gestational age at which the developmental failure or insult occurred (Table).

Page 694
It is essential to perform high-resolution CT to confirm the diagnosis of semicircular canal aplasia. Aplasia and fibrous or calcified obliteration of the canals have the same appearance at MR imaging. However, at CT, the semicircular canal is absent in cases of aplasia, whereas a normal canal is seen in cases of fibrous obliteration (since fibrous tissue cannot be seen at CT) and calcifications within the canal are seen in cases of labyrinthitis ossificans (5).

Page 696
The morphologic characteristics and size of the IAC are not reliable indicators of the integrity of the cochlear nerve, and normal size of the IAC and normal inner ear anatomy do not exclude a nerve deficiency; the nerve may even be absent when the IAC and labyrinth are completely normal. Hence, high-resolution MR imaging is the preferred modality for accurate assessment of the cochlear nerve (23).

Page 697 (Figure on page 696)
The discrete foci of white-matter signal abnormality that are frequently seen on MR images obtained in children with sensorineural hearing loss (Fig 13b) have been attributed to cytomegalovirus infection at birth (27,28).